

## INFLUENCE OF DEFORMATION ON THE COATING PROPERTIES OF AIRCRAFT FUSELAGE SHELLS

<sup>1</sup>Jan JEPKENS, <sup>1</sup>Norman HEIMES, <sup>1</sup>Hendrik WESTER, <sup>1</sup>Philipp MÜLLER, <sup>1</sup>Sven HÜBNER,  
<sup>2</sup>Simon WEHRMANN, <sup>2</sup>Matthias MÜLLER, <sup>1</sup>Bernd-Arno BEHRENS

<sup>1</sup>IFUM - Leibniz University Hannover, Hannover, Germany, EU, [jepkens@ifum.uni-hannover.de](mailto:jepkens@ifum.uni-hannover.de),  
[heimes@ifum.uni-hannover.de](mailto:heimes@ifum.uni-hannover.de), [wester@ifum.uni-hannover.de](mailto:wester@ifum.uni-hannover.de), [mueller@ifum.uni-hannover.de](mailto:mueller@ifum.uni-hannover.de),  
[huebner@ifum.uni-hannover.de](mailto:huebner@ifum.uni-hannover.de), [behrens@ifum.uni-hannover.de](mailto:behrens@ifum.uni-hannover.de)

<sup>2</sup>Deharde GmbH, Varel, Germany, EU, [s.wehrmann@deharde.de](mailto:s.wehrmann@deharde.de), [m.mueller@deharde.de](mailto:m.mueller@deharde.de)

<https://doi.org/10.37904/metal.2023.4659>

### Abstract

Manufacturers like Airbus have strict specifications concerning the process sequence of fuselage shell forming. Coating may only take place after forming, because conventional processes induce large deformation which could cause coating failure. A novel incremental bending process known as Deharde Polygon Forming<sup>®</sup> (DPF<sup>®</sup>), has the potential to challenge existing process sequence restrictions due to lower deformations. Thus, it is to be investigated if precoated sheets can be formed by DPF<sup>®</sup> with regard to the coating properties. Correspondingly, in the scope of this work, starting from the initial state of coated EN AW - 2024 - T351, the changes of the Seevenax-313-81 coating after preloading were analysed. Therefore, three different strain states were induced by Marciniak tests and scaled fuselage shells were produced by DPF<sup>®</sup> from which specimens were obtained. Afterwards, the evolution of coating properties such as hardness, Young's modulus, elastic and plastic behaviour and friction coefficient were investigated by scratch and indentation tests with a Triboindenter TI 950. In parallel, the formed specimens were analysed for coating failure by using integrated optics. It was found, that the pre-stretched specimens by Marciniak tests and scaled DPF<sup>®</sup> do not undergo significant changes in the application characteristics of the coating. However, the former was found to have cracks in the coating. In contrast, for scaled DPF<sup>®</sup> fuselage shells, where compressive stresses are induced by contact with the tool or spring steel package, no failure were detected in the surface of the coating. The results indicate potential for flexibilization of the process chain regarding forming and coating.

**Keywords:** Coating properties, nanoindentation, Marciniak tests, incremental bending, fuselage shells

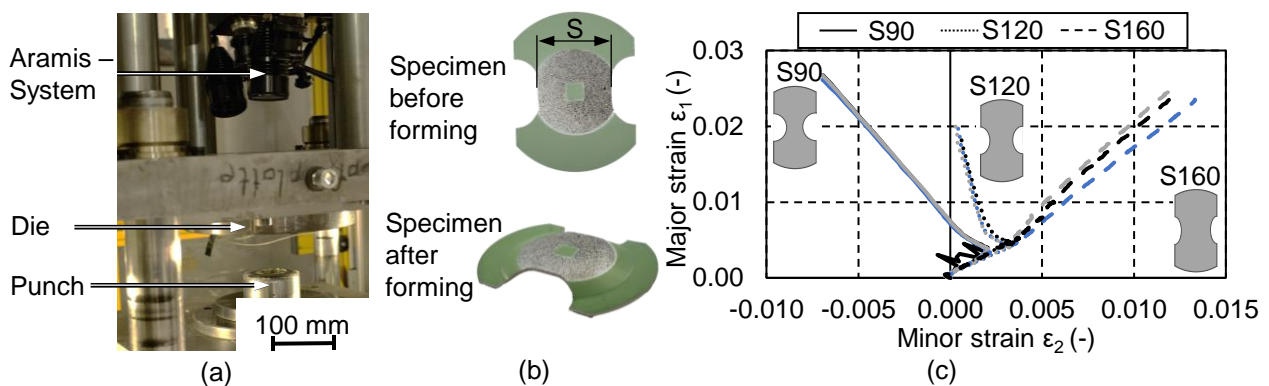
### 1. INTRODUCTION

The fuselage of aircraft such as Airbus's A320 series is still mainly made from aluminium alloys [1]. Precipitation hardenable aluminium alloys such as the 7000 and 2000 series are used for this purpose [2]. Due to a heterogeneous microstructure, a high strength-to-weight ratio is achieved. In parallel, such alloys are susceptible to corrosion due to their microstructure [3]. Especially for the operating conditions in aviation with fluctuating temperatures and chemical contact to different substances, a reliable passive corrosion protection is necessary [4]. Hence, aluminium alloys are coated with a system consisting of an anodizing layer, a primer and a top-coating [5]. Stability and durability of the mentioned corrosion protection over the entire lifecycle of aircrafts is a requirement to ensure safe operation [4]. Therefore, Original Equipment Manufacturer (OEM) such as Airbus have strict specifications with regard to the coating. Accordingly, the process sequence for coating and peripheral processes is determined, in order to prevent forming of coated sheets [6]. A reason for the restrictions is that the induced stresses and strains in conventional forming processes could cause coating failure. This can be inferred from the study by Peng et al. where significant major stresses and thinning during stretch forming of fuselage shells were numerically predicted even for a low sheet thickness of 1.6 mm [7].

According to Panton et al., another conventional process such as roll forming can be characterised by a superposition of different stress states including significant shear stresses, that are induced by the relative movement between tool and workpiece [8]. Furthermore, it is evident that the lower yield point in the tangential stress state enhances plastic deformation. Thus, the presented investigations confirm the existing restrictions with regard to the process sequence for the forming of fuselage shells with conventional processes. According to the specification AIPI02-001-003 the anodizing process includes the use of environmentally harmful alkalis and acids [6]. The consumption of these fluids depends on the geometry to be anodized. Consequently, the necessary demand for the treatment of already formed fuselage shells exceed that for plane sheets several times. Therefore, forming of coated sheets can significantly reduce the consumption of environmentally harmful fluids. Since Deharde Polygon Forming<sup>®</sup> (DPF<sup>®</sup>) was patented in 2020, an incremental bending process exists that is capable to form fuselage shells by inducing lower strains per increment [9]. Due to the incremental character of the DPF<sup>®</sup>, the current restrictions can be reconsidered. Following Zhang et al., current research is primarily focused on the environmental effects of aviation on the coating and the optimization of coating materials [10]. In contrast to the current state of the art, this paper investigates the effects of forming on the mechanical properties of a coating. For this purpose, the specimens were first preloaded using the Marciniak test and DPF<sup>®</sup>. Then the evolution of coating properties such as hardness, Young's modulus, elastic and plastic behaviour and coefficient of friction were investigated by scratch and indentation tests using a triboindenter.

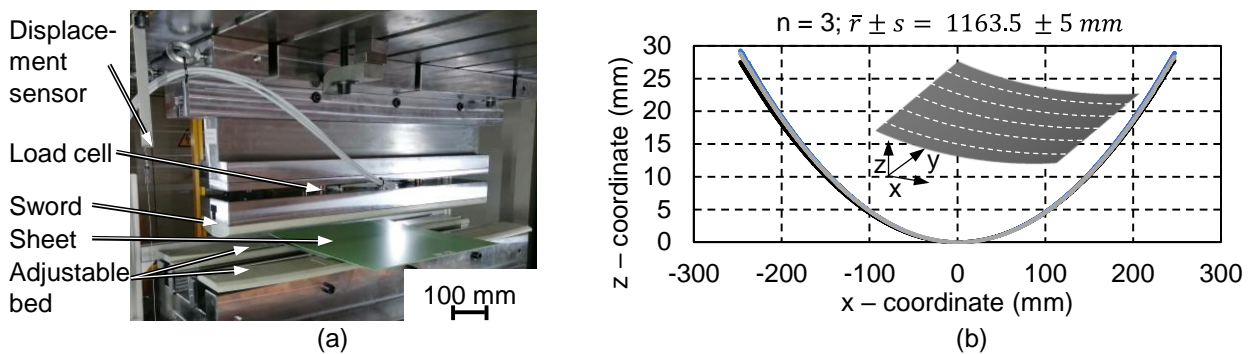
## 2. MATERIALS AND METHODS

The investigations were carried out on the aluminium-copper alloy EN AW -°2024 - T351 with Seevenax-313-81 coating (**primer**) and a thickness of 3.36 mm. For this purpose, the design of Marciniak specimens and tool are shown in **Figure 1** (a) The experimental procedure was conducted in accordance with DIN EN ISO 12004-2 [11]. Due to the sheet thickness and the necessary blank holder force a hydraulic double-column press type HD 250 from Dunkes GmbH was used. Path-controlled preloading of the water jet cut Marciniak specimens with widths of  $S = 90$  mm and 120 mm was applied by draw depths of 14 mm at a velocity of 2 mm/s and room temperature. Experiments of  $S = 160$  mm specimens were performed to a drawing depth of 20 mm. Specimen geometry and draw depths were selected based on experience from literature and numerical simulation for approximation of strain states in incremental bending. For the preloading of the Marciniak specimens, the generated strain states were measured in the homogeneous region by means of digital image correlation (**DIC**) with an aramis system from Carl Zeiss GOM Metrology GmbH. During previous application of stochastic pattern by spray paint for strain measurement, the examination area for nanoindentation was covered, shown in **Figure 1** (b), to ensure a paint-free subsequent measurement with a triboindenter. In **Figure 1** (c), three strain states are shown based on three measurements each in succession to the preload.



**Figure 1** (a) Setup Marciniak test; (b) Specimen preparation for DIC; (c) Measured resulting strain paths induced by Marciniak tests

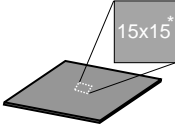
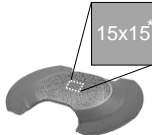
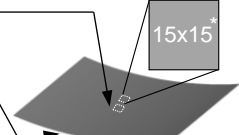
In order to additionally analyse a more process-oriented strain state, coated sheets were bent incrementally to scaled fuselage shells by DPF<sup>®</sup>. For this purpose, the tool from **Figure 2** (a) containing the active parts sword and bed made of polypropylene with radii of 215 mm and 12 mm were used. A three-layer spring steel package of 1.1274 with a sheet thickness of 1.5 mm each and a total dimension of 510 mm x 300 mm x 4.5 mm was positioned on the bed to enable forming of the edges. To ensure repeatable positioning and forming the spring steel package was provided with a centre line. Furthermore, relative orientation to the bed was marked on the latter. As the coated specimen with a dimension of 500 mm x 500 mm x 3.36 mm was placed on the spring steel package, the feed was manually controlled by means of appropriate markers every 20 mm. Tooling was placed in a hydraulic press Dunkes type HDZ 400, which performed the strokes path-controlled at a speed of 10 mm/s. Experimental tests were carried with a bed width of 132 mm up to a bottom dead centre of -0.8 mm. After incremental bending scaled fuselage shells were measured optically using ATOS 2 400 system from Carl Zeiss GOM Metrology GmbH. Based on five cross sections, the averaged inner radius  $r$  and standard deviation  $s$  were determined on  $n = 3$  specimens, whose mid cross-section and averaged inner radius of 1163.5 mm are shown in **Figure 2** (b). The cross sections were defined using a local coordinate system and are located on the symmetry line as well as  $\pm 100$  and  $\pm 200$  mm from it in  $y$  - direction.



**Figure 2** (a) Setup scaled DPF<sup>®</sup> tool; (b) Mid cross-section of scaled fuselage shell

After preloading, the examination zone of the Marciniak specimen and two central specimens for inner side (IS) and outer side (OS) were extracted from the scaled fuselage shells with dimensions of 15 x 15 mm<sup>2</sup> by water jet cutting. To characterise the mechanical and tribological properties of the preloaded coating, the specimens from **Table 1** were examined on the Hysitron Triboindenter TI 950. A Berkovich diamond tip with a tip radius of 100 nm was used to determine the mechanical properties such as nano hardness and Young's modulus. The area function of the Berkovich tip was calibrated on fused quartz and a minimum penetration depth of 40 nm was determined. For each variant from **Table 1**, the specimens were examined at nine different measuring positions. A field of 5x5 indents with a spacing of 5  $\mu$ m was set up at each measuring position. A trapezoidal function was selected as load function with a maximum test force of 300  $\mu$ N following Heimes et al. [12]. In addition to the investigations on the surface of the coating, an initial specimen was also examined in cross-section in order to be able to characterise the interface between primer and EN AW - 2024 - T 351.

**Table 1** Type, origin and number of specimens for examination with the Triboindenter

Initial State	Marciniak Specimen	DPF <sup>®</sup>
$n = 3$ 	S90, S120 and S160 Outer side $n = 3$ each 	Inner side Outer side $n = 3$ each 
*All dimensions in mm		

A conical diamond tip with a tip radius of 300 nm was used for to characterise the elastic and plastic material behaviour and the tribological behaviour of the coating. Nine scratch tests were carried out for each variant. In the scratch test, the normal force was increased linearly from 2  $\mu\text{N}$  to 50  $\mu\text{N}$  over the scratch length of 8  $\mu\text{m}$  and recorded. The detailed procedure of the scratch test can be found in Behrens et al. [13]. From the scratch test results, the ratio of the elastic fraction was calculated as the difference between scratch and postscan and the plastic fraction as the difference of pre- and postscan. In parallel, the formed specimens were analysed for coating failure by integrated optics. Additionally, images of the initial state were taken in transverse and cross-sections using a light microscope Polyvat Met from Reichert and Jung. Subsequently, the thickness of the anodization layer and the primer were measured using analyseSIS docu v5.2 from Olympus. Finally, the microstructure in the barked sections were qualitatively analysed.

### 3. RESULTS AND DISCUSSION

The analysed thicknesses of primer and anodization layer in the initial state, are shown in **Figure 3** (a). It is evident that the measured values for the primer of 32.95  $\mu\text{m}$  and 34.85  $\mu\text{m}$  are above the range of 15 to 25  $\mu\text{m}$  required by Airbus [14]. In contrast, the anodization layer of 2.65  $\mu\text{m}$  meets the specification [6]. Contextualizing the microstructure from **Figure 3** (b) and the hardness mapping from **Figure 3** (c), it follows that the anodization layer has the highest nano hardness  $H$  of about 6 GPa, whereas the primer has only a low hardness below 1.75 GPa. In parallel, the results indicate that a decrease in nano hardness of the aluminium is associated with formation of coarse grains below the anodization layer.

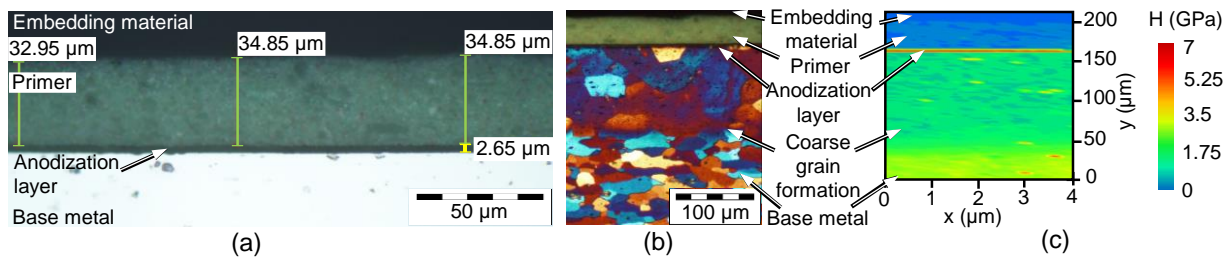


**Figure 3** (a) Thickness of primer and anodization layer; (b) microstructure; (c) nano hardness  $H$  mapping for cross section in the initial state

**Figure 4** shows on one hand in (a) the nano hardness and on the other hand in (b) the Young's modulus evolution of the primer due to the applied pre-strains by Marciniak test and DPF<sup>®</sup> for IS and OS as well as the initial state. Accordingly, the median of hardness increases significantly by 11 to 23 % compared to the initial state. The Young's modulus median, however, undergoes only marginal changes. An exception is the S90 Marciniak specimen, where an increase in the median of 9 % is present. In Addition, the spread of the mentioned values increases due to preloading.

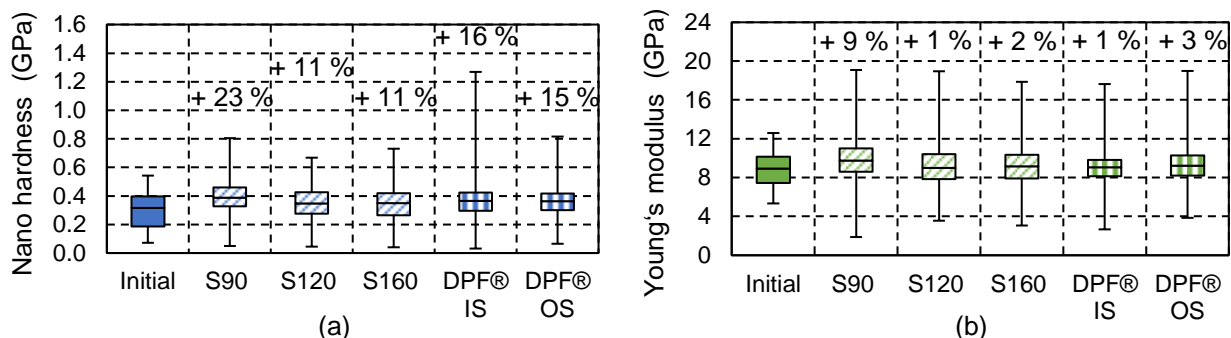


**Figure 4** Boxplots of (a) Nano hardness and (b) Young's modulus before and after forming



Moreover, an examination of the surfaces is presented in **Figure 5** (a), that already has a large amount of pores in the initial state. Exemplified for the stretch forming strain state by S90 Marciniak specimen with the largest increase in nano hardness and Young's modulus, crack formation over several pores occurs. In contrast, **Figure 5** (b) and (c) depict that no cracks can be detected for scaled fuselage shells, where the stress state near the surface is superimposed by compression, due to tool contact.

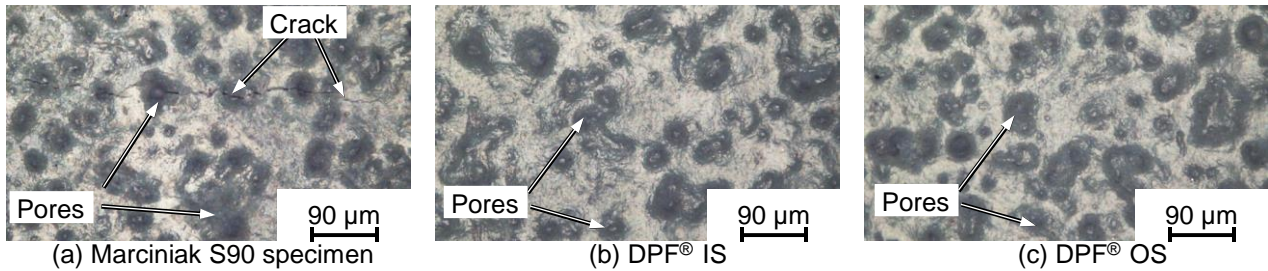


**Figure 5** Image of the preloaded surfaces from integrated optics of the Triboindenter

Due to the crack formation in the Marciniak specimens, the presentation of the elastic and plastic ratios as well as coefficient of friction (CoF) in **Figure 6** (a) is limited to the initial state and the scaled fuselage shells. Compared to the initial state, the CoF on the pressure-superimposed tensile stressed OS undergoes no significant change. On the pressure-superimposed IS subjected to compressive stress, the CoF increases by approximately 62 %. This can be explained by residual tensile stresses that remain on IS after springback during bending [15]. As a result, the contact area, the lateral force and the CoF increase. Furthermore, the coating on the IS shows increased plastic ratios while the OS has lower plastic ratios compared to initial state, due to the remaining residual tensile stresses on IS and residual compressive stresses on OS [15]. However, the results of the elastic and plastic ratios show significant standard deviations. One reason for this are the large penetration depths exemplified by the prescan, scratch and postscan for the IS of scaled fuselage shells, shown in **Figure 6** (b). However, this could be explained by the analysis of surfaces with technical roughness, in contrast to the methodology of Behrens et al. where polished surfaces are investigated [13].

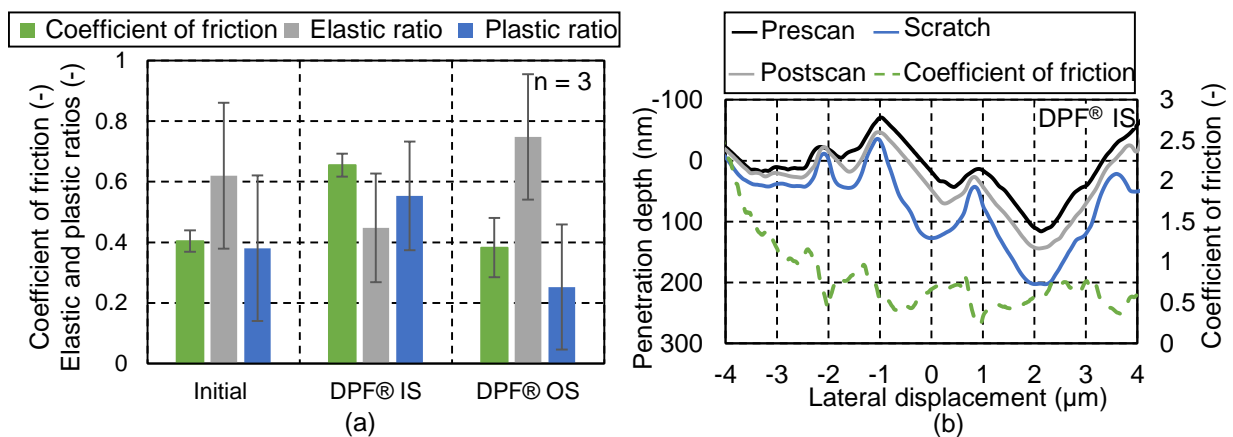


**Figure 6** (a) Elastic and plastic coating behaviour and coefficient of friction; (b) Scratch test of DPF® IS

#### 4. CONCLUSION AND OUTLOOK

Finally, the following conclusions can be drawn from the presented study. Anodizing results in grain growth and decrease in nano hardness of the base metal immediately below the anodizing layer. In parallel, the anodization layer has the largest nano hardness compared to primer and base metal. By preloading of the Marciniak and DPF® specimen a beneficial increase in nano hardness of the primer is caused, whereas Young's modulus remains constant after preloading for most strain states. The only exception was observed

for the S90 Marciniak specimens for the stretch forming strain state. In addition, it should be stated that DPF<sup>®</sup> has the advantage of inducing additional pressure on the surface through contact with the spring steel package on OS and the sword on IS. As a result, compared to the outside of the Marciniak specimens cracking can be avoided. Therefore, the presented analyses suggest that DPF<sup>®</sup> is suitable for forming precoated sheets. However further investigations are necessary to analyse the effect of forming on resulting corrosion behaviour by artificial corrosion and aging tests.

## ACKNOWLEDGEMENTS

**The paper was obtained within the collaborative project “Aggregated Polygon Forming based Processes for large Fuselage Components” (ZW1-80159743), funded by the Investitions- und Förderbank Niedersachsen - NBank. The authors gratefully acknowledge NBank for their financial support.**

## REFERENCES

- [1] DURSUN, T., SOUTIS, C. Recent developments in advanced aircraft aluminium alloys. *Materials & Design*. 2014, vol. 56, pp. 862-871.
- [2] MÜLLER, P., BEHRENS, B.-A., HÜBNER, S., JEPKENS, J., WESTER, H., LAUTENBACH, S. Development of polygon forming processes for aerospace engineering. In: *Materials Research Proceedings*. Erlangen: Materials Research Forum, 2023, pp. 69-76.
- [3] HUGHES, A. E., BIRBILIS, N.; MOL, J. M. C., GARCIA, S. J., ZHOU, X., THOMPSON, G.E. High Strength Al-Alloys: Microstructure, Corrosion and Principles of Protection. In *Recent Trends in Processing and Degradation of Aluminium Alloys*. Rijeka, InTech, 2011.
- [4] PAZ MARTINEZ-VADEMONTE, M., ABRHAMI, S.T., HACK, T., BURCHARDT, M. TERRY, H. A Review on Anodizing of Aerospace Aluminum Alloys for Corrosion Protection. *Coatings*. 2020, vol. 10, pp. 1106-1135.
- [5] PELTIER, F., THIERRY, D. Review of Cr-Free Coatings for the Corrosion Protection of Aluminum Aerospace Alloys. *Coatings*. 2022, vol. 12, pp. 518 - 544.
- [6] AIPI02-01-003. *AIPI Airbus Process Instruction: Tartaric Sulphuric Anodizing of aluminum alloys for corrosion protection and paint pre-treatment*. AIRBUS Operations S.A.S., 2020.
- [7] PENG, J., LI, W., HAN, J., WAN, M., MENG, B. Kinetic locus design for longitudinal stretch forming of aircraft skin components. *International Journal of Advanced Manufacturing Technology*. 2016, vol. 86, pp. 3571-3582.
- [8] PANTON, S.M., DUNCAN, J.L., ZHU, S.D. Longitudinal and shear strain development in cold roll forming. *Journal of Materials Processing Technology*. 1996, vol. 60, pp. 219-224.
- [9] BLAZEK, I., BRESTRICH, M., FRERICHS, H., HARMS, M., LAUTENBACH, S., EILERT, W. Method and arrangement for changing the shape of a sheet-like workpiece. European Patent No. 2019050955, 2020.
- [10] ZHANG, T., ZHANG, T., HE, Y., WANG, Y., BI, Y. Corrosion and aging of organic aviation coatings: A review. *Chinese Journal of Aeronautics*. 2022, vol. 36, pp. 1-35.
- [11] DIN EN ISO 12004-2. *Metallic materials - Determination of forming-limit curves for sheet and strip - Part 2: Determination of forming-limit curves in the laboratory*. Berlin: Beuth Verlag GmbH, 2021.
- [12] HEIMES, N., PAPE, F., KONOPKA, D., SCHÖLER, S., MÖHWALD, K., POLL, G., BEHRENS, B.-A. Investigation of the Scaling of Friction Coefficients from the Nano to the Micro Level for Base Materials and Coatings. In *Production at the leading edge of technology*. Berlin, Heidelberg: Springer, 2021, pp. 161-170.
- [13] BEHRENS, B.-A., POLL, G., MÖHWALD, K., SCHÖLER, S., PAPE, F., KONOPKA, D., BRUNOTTE, K., WESTER, H., RICHTER, S., HEIMES, N. Characterization and Modeling of Nano Wear for Molybdenum-Based Lubrication Layer Systems. *Nanomaterials*. 2021, vol. 11, pp. 1363-1386.
- [14] 80-T-35-5030 *Beiblatt 6: Coating with two-/three- component water based primer - Product Seevenax 313-81 (2k-Version)* Airbus, 2021.
- [15] ESSA, A., NASR, M., AHMED, M. Variation of the residual stresses and springback in sheet bending from plane-strain to plane-stress condition using finite element. *The International Conference on Applied Mechanics and Mechanical Engineering*. 2016, vol. 17, pp. 1-14.